NOTES AND CORRESPONDENCE

Stable Shallow Water Vortices over Localized Topography

ROBERTO IACONO

ENEA, C.R. Casaccia, Rome, Italy

(Manuscript received 8 September 2009, in final form 18 November 2009)

ABSTRACT

It is shown that a sufficient condition for stability by P. Ripa, based on the monotonicity of the flow potential vorticity (PV), can be used to prove linear stability of isolated shallow water vortices over localized topographic features. Stable axisymmetric vortices over axisymmetric topography that satisfy Ripa's condition are explicitly constructed by using a simple two-step, fully analytic approach. First, for a given velocity profile, the topography is found that yields a steady-state, constant-PV solution of the shallow water equations. Then, this topography is slightly modified to obtain new steady solutions, with monotonic PV, that satisfy Ripa's stability criterion. Application of this procedure shows that modest depressions (elevations) can stabilize cyclones (anticyclones) with small Rossby and large Burger numbers and velocity profiles similar to those observed in mesoscale oceanic vortices. The stabilizing topographic features have radial sizes comparable with that of the vortex (about twice the radius of maximum speed) and maximum vertical size, normalized to the unperturbed fluid depth, from 2 to 3.3 times the Rossby number for the profiles considered. The upper limit corresponds to a Gaussian profile, whereas the lower limit is approached by a velocity profile that is linear inside the vortex core and a cubic polynomial outside.

Finally, it is argued that a similar stabilization mechanism holds for two-dimensional (2D) flows, and a method for the construction of stable 2D shallow water vortices over 2D topography is outlined that is analogous to that used for the axisymmetric problem. In the 2D case, however, it is generally not possible to obtain stable equilibria analytically.

1. Introduction

The stability of oceanic vortices over isolated topography has been investigated by Nycander and LaCasce (2004, hereafter NL04) in the context of the two-dimensional (2D) inviscid Euler equation in a nonrotating environment. The main result of NL04 is that there is a large class of stable, stationary anticyclonic vortices attached to seamounts (quite wider than that found in the classical investigation by Carnevale and Frederiksen 1987), whereas stable cyclones can only exist over axisymmetric topographic features. This asymmetric behavior could contribute to explain the fact that some observed seamounts do possess stationary anticyclonic caps (see, e.g., the case of the Fieberling Seamount, which was studied by Kunze and Toole 1997).

Corresponding author address: Dr. Roberto Iacono, ENEA, C.R. Casaccia, Via Anguillarese 301, Rome 00123, Italy.
E-mail: roberto.iacono@enea.it

DOI: 10.1175/2009JPO4357.1

However, the dynamical setting of NL04 is very simplified and one may wonder about the robustness of the stability results. For example, the recent work of Benilov (2005) indicates that the stability picture may be significantly modified by baroclinic effects. Other potentially important limitations, also present in the approach of Benilov (2005), are the inherent restrictions to small-amplitude topographic features and quasigeostrophic dynamics. As a first step toward the removal of these limitations, here we examine stability of vortices over topography in the context of the shallow water (SW) model, which allows both for finite-amplitude topography and for ageostrophic effects. Our objective is not a thorough investigation of the SW stability problem, which would require extensive numerical work. We seek, instead, to gain analytic insight by exploiting a somewhat neglected stability criterion for the SW equations (SWE) by Ripa (1987) that is based on the monotonicity of the flow potential vorticity (PV).

Ripa's stability condition, originally derived for flows over a flat bottom, has not proven very useful in that

context, since it only applies to circular flows and moreover cannot be satisfied by isolated circular vortices (Nore and Shepherd 1997). Interestingly, however, the condition also holds for flows over arbitrary bathymetry. This result is implicitly stated in Ren and Shepherd (1997), which is concerned with the derivation of an analog of Ripa's stability condition for Salmon's (1983) balance model. It is noted in that work that the pseudoenergy functional that yields the stability criterion [their Eq. (3.9)] is formally identical to that for the SWE, once the geostrophic velocity is replaced by the full velocity vector. Since the derivation of Ren and Shepherd (1997) is for flows over variable topography, in general geometry, this implies that Ripa's stability criterion for the SWE holds for the same conditions. This fact, perhaps not widely appreciated, is easily understood by observing that a variable bottom topography only affects the equilibrium state but not the conservation laws of energy and PV that lead to the stability criterion.

Since the negative argument by Nore and Shepherd (1997) does not hold in the presence of topography, this may allow existence of axisymmetric, isolated SW vortices over appropriate axisymmetric topographic features that satisfy Ripa's condition. On the other hand, in the presence of nonaxisymmetric topography, the restriction to circular flows would be waived, and it might be possible to find 2D SW vortices over 2D topography that are stable according to Ripa's criterion. The main purpose of this work is to examine these possibilities, which apparently have not been explored in the literature.

The stability of SW axisymmetric equilibria is discussed in section 2, where we analytically construct isolated vortices with realistic velocity profiles (e.g., Gaussian vortices), trapped on localized topographic features, that satisfy Ripa's condition. In section 3, an analogous, more elaborate construction is outlined that allows, in principle, stable two-dimensional SW vortices over two-dimensional topography to be obtained. Conclusions are drawn in section 4, where the main limitations of the present analysis are reminded and some directions for future work are indicated.

2. Stability of axisymmetric SW vortices

We first investigate the stability of axisymmetric SW vortices over axisymmetric topographic features. In particular, we consider isolated axisymmetric vortices: that is, vortices with an azimuthal velocity profile $V(r)$ that decays more rapidly than $1/r$ at large r. For such flows, Ripa's condition ensures stability against small-amplitude perturbations if

$$V\frac{dq}{dr} > 0, \quad V^2 < gh \tag{1}$$

for any r. Here, q is the PV; h is the fluid depth; and g is the acceleration due to gravity, or the "reduced" gravity in a 1 + ½ layer context. In the following, we shall construct isolated SW vortices over topography that satisfy (1), using a simple two-step approach: first, given a velocity profile, we shall determine the topography needed to make this profile a steady, constant-PV solution of the SWE; then, with slight modifications of this topography and of the corresponding fluid depth, we shall obtain new steady solutions that satisfy Ripa's condition for stability. For simplicity, although it is not fully appropriate, we shall denote the topography corresponding to constant PV as the "marginal topography."

In an axisymmetric configuration, the basic equilibrium relations are the radial force balance,

$$g\frac{d}{dr}(h + h_b) = fV + \frac{V^2}{r}, \tag{2}$$

and the definition of the PV,

$$q = \frac{\zeta + f}{h}, \tag{3}$$

with $h_b(r)$ the height of the bottom topography, $\zeta = dV/dr + V/r$ the relative vorticity, and f the Coriolis parameter that is taken to be constant and positive throughout the paper. Computing the fluid depth gradient from (3),

$$\frac{dh}{dr} = \frac{1}{q}\frac{d\zeta}{dr} - \frac{\zeta + f}{q^2}\frac{dq}{dr}, \tag{4}$$

and placing it in (2) gives a useful expression for the PV gradient,

$$(\zeta + f)\frac{dq}{dr} = q\frac{d\zeta}{dr} - \frac{q^2}{g}\left(fV + \frac{V^2}{r}\right) + \frac{dh_b}{dr}q^2. \tag{5}$$

Consider a cyclonic vortex over flat bottom (i.e., $dh_b/dr = 0$), with a velocity profile that peaks at some radius R. It is easily seen that, for such a vortex, the rhs of (5) is negative definite in a neighborhood of $r = R$ (note that $d\zeta/dr < 0$ at the velocity maximum). It follows that Ripa's condition is always violated in the region of maximum velocity of a cyclonic vortex, unless a positive topographic slope is present in that area [see the last term in (5)] that is strong enough to change the local sign of the PV gradient. Similar considerations pertain to the flow in the region of minimum velocity of an anticyclonic vortex, as long as $|\zeta(R)|/f$ is smaller than unity. In that case, the "stabilizing" topography would be hill-like.

If we set $q = \tilde{q} = f/H$, with H the unperturbed fluid depth [i.e., $H = h(r \to \infty)$], and denote the marginal topography by $\tilde{h}_b$, (5) reduces to

$$\frac{d\tilde{h}_b}{dr} = -\frac{H}{f}\frac{d\zeta}{dr} + \frac{1}{g}\left(fV + \frac{V^2}{r}\right). \tag{6}$$

Integrating this relation and choosing the integration constant so that $\tilde{h}_b$ vanishes at infinity, we finally get

$$\frac{\tilde{h}_b(r)}{H} = -\frac{\zeta(r)}{f} - \frac{1}{gH}\int_r^\infty dr\left(fV + \frac{V^2}{r}\right), \tag{7}$$

which gives the marginal topography for any $V(r)$ profile of interest. The corresponding fluid depth $\tilde{h}$ follows from (3),

$$\frac{\tilde{h}(r)}{H} = 1 + \frac{\zeta(r)}{f}. \tag{8}$$

The first step accomplished, we must now show that stable vortices can be obtained through appropriate modifications of the marginal topography profile. To this end, it is sufficient to notice that, since the radial force balance only involves the free surface elevation $h + h_b$, infinite steady states correspond to any given $V(r)$, characterized by the couples of profiles $[h(r), h_b(r)]$ such that $h + h_b$ is a solution of (2). The constant-PV vortex defined by (7) and (8) is just one of these couples; any other vortex with the same $V(r)$ and

$$h = \tilde{h} - \gamma(r), \quad h_b = \tilde{h}_b + \gamma(r) \tag{9}$$

(with γ vanishing at large r and such that h is nonnegative) belongs to the same class of steady states, whose PV is given by

$$q = \tilde{q}\frac{1}{1 - \gamma/\tilde{h}}. \tag{10}$$

In this class, solutions with monotonic PV can be selected by choosing $\gamma(r)$ so that $\gamma(r)/\tilde{h}$ is monotonic. For example, we can choose

$$\gamma(r) = -\epsilon\tilde{h}e^{-r/R}, \tag{11}$$

with ϵ a constant, so that

$$q = \tilde{q}\frac{1}{1 + \epsilon e^{-r/R}}, \quad h_b = \tilde{h}_b - \epsilon\tilde{h}e^{-r/R}. \tag{12}$$

Since $|\epsilon|$ can be taken as small as wanted, we can construct topographic profiles arbitrarily close to $\tilde{h}_b$ that yield solutions with a sign definite dq/dr. In particular, we can construct topographic profiles arbitrarily close to $\tilde{h}_b$ for which (1) is satisfied. Since dq/dr has the same sign of ϵ, (12) shows that cyclones satisfying (1) are obtained for positive ϵ: that is, by slightly deepening the marginal topography. Similarly, stable anticyclones are obtained for $\epsilon < 0$: that is, by making the underlying elevation slightly taller.

Clearly, we are assuming here that the second condition in (1) can be fulfilled, through an appropriate choice of the flow Froude number. Indeed, it follows from (8) that the marginal flow satisfies this condition if

$$\frac{V_m^2}{gH} < \min\left[\frac{1}{v^2}\left(1 + \frac{\zeta}{f}\right)\right]; \quad \frac{\zeta}{f} = \frac{\omega_m}{f}\left(\frac{dv}{dx} + \frac{v}{x}\right), \tag{13}$$

where we have introduced the normalizations $x = r/R$ and $v = V/V_m$, with V_m the (signed) velocity extremum, and defined $\omega_m \equiv V_m/R$. Since

$$\frac{V_m^2}{gH} = \left(\frac{\omega_m}{f}\right)^2\left(\frac{R}{\sqrt{gH}/f}\right)^2 = \frac{(\omega_m/f)^2}{(L/R)^2},$$

with $L \equiv \sqrt{gH}/f$ the deformation radius, (13) can also be seen as a constraint on the ratio between the square of the Rossby number $\mathrm{Ro} \equiv \omega_m/f$ and the Burger number $\mathrm{Bu} \equiv (L/R)^2$. At small Ro, this ratio cannot exceed a value that is of order unity, the exact bound depending on the velocity profile in consideration.

Before discussing explicit examples, we may further examine the expression for the marginal topography. With the normalizations just introduced, (7) takes the form

$$\frac{\tilde{h}_b(r)}{H} = -\frac{\zeta(r)}{f} - \frac{1}{(L/R)^2}\left[\frac{\omega_m}{f}\int_x^\infty dx\, v + \left(\frac{\omega_m}{f}\right)^2\int_x^\infty dx\,\frac{v^2}{x}\right], \tag{14}$$

which explicitly shows the dependencies on the Rossby and Burger numbers, the two parameters of the problem. When Bu is much larger than unity and $|\zeta|$ is maximum in the vortex core, the rhs of (14) is dominated by the first term. The corresponding marginal topography for an anticyclonic (cyclonic) vortex is a hill (valley) with shape close to that of the $-\zeta(r)/f$ profile and maximum size (normalized to H) on the order of the dynamical Rossby number $|\zeta(0)|/f$.

For Bu of order unity, the Coriolis term in (14) becomes nonnegligible. Since this term has the same sign as the first one, it always tends to increase the size of the marginal topographic feature. On the other hand, the centrifugal term is negative definite and always tends

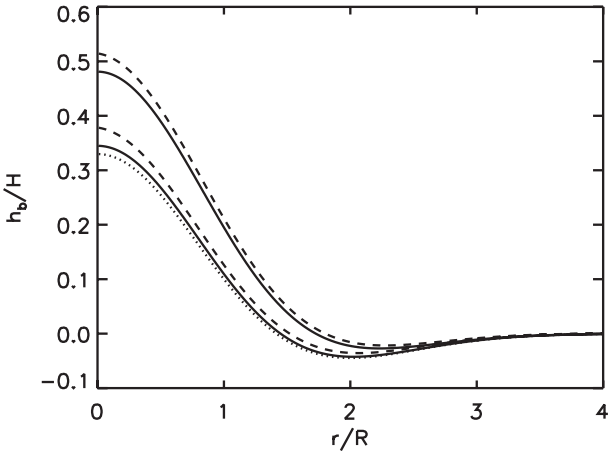

FIG. 1. The solid lines are the marginal topography profiles (see the text for definition) for two Gaussian vortices, with Rossby number equal to −0.1 and Burger numbers of 1 (top line) and 10 (bottom line; the dotted line gives the $-\zeta/f$ profile for both vortices). Also shown (dashed lines) are modified topography profiles that yield stable solutions of the SWE.

to reduce the marginal topographic height, thereby introducing an asymmetry between cyclones and anticyclones that favors the latter. It should be noted, however, that this term becomes a significant fraction of the Coriolis term only for large values of Ro that imply marginal topographic features of unrealistic sizes (see the examples below). At moderate Ro, the asymmetry could be somewhat amplified by taking small Bu; then, however, (13) may become a limitation. Therefore, to have realistic topographic features and to satisfy both the conditions required for stability, in the following we shall restrict to flows with small Ro as well as Bu of order unity or larger for which the asymmetry between cyclones and anticyclones is small.

Examples of stable vortices

Let us now consider specific examples. We start with a Gaussian velocity profile: that is, $V(r) \propto r \times \exp(-\lambda r^2)$, with λ a constant, which is often used in theoretical work and is sometimes used to fit observations of oceanic vortices (see, e.g., the meddy described by Paillet et al. 2002). The stability of these vortices over a flat bottom, in the context of the SWE, has been studied numerically by Stegner and Dritschel (2000; in fact, they examined a wider class of vortices, with both steeper and broader vorticity profiles). In the limit of large Burger number (see Stegner and Dritschel 2000, their Fig. 3), Gaussian vortices, both cyclonic and anticyclonic, were found to be unstable, independently from the Rossby number and consistently with the quasigeostrophic results of Carton et al. (1989). Here, we show that these vortices can be stabilized by topography.

For a Gaussian vortex,

$$v = x\exp\left[\frac{1}{2}(1-x^2)\right], \quad \zeta = \zeta_0\left(1-\frac{x^2}{2}\right)\exp\left(-\frac{1}{2}x^2\right), \tag{15}$$

where $\zeta_0 \equiv \zeta(0) = 2\sqrt{e}\omega_m$. Placing (15) in (14) and evaluating the integrals, we find

$$\frac{\tilde{h}_b}{H} = -\frac{\omega_m}{f}\left[2\left(1-\frac{x^2}{2}\right)+\left(\frac{R}{L}\right)^2\right]\exp\left[\frac{1}{2}(1-x^2)\right] - \frac{1}{2}\left(\frac{\omega_m}{f}\right)^2\left(\frac{R}{L}\right)^2\exp(1-x^2). \tag{16}$$

The corresponding fluid depth is

$$\frac{\tilde{h}}{H} = 1+\frac{\zeta_0}{f}\left(1-\frac{x^2}{2}\right)\exp\left[\frac{1}{2}(1-x^2)\right]. \tag{17}$$

Figure 1 shows the $\tilde{h}_b/H$ profiles for two anticyclonic vortices with Ro = −0.1 and Bu = 1 and 10. As expected, the marginal topography for the latter vortex (lower solid curve) has a shape close to that of $-\zeta/f$ (dotted line), with a central normalized height close to the dynamical Rossby number (about 0.33). In the case with Burger number equal to unity (upper solid line), the correction resulting from the Coriolis term becomes relevant and increases the marginal topography. The dashed lines in the same figure are modified topography profiles, with γ chosen as in (11) and $\epsilon = -0.05$, that correspond to solutions satisfying Ripa's condition. It may be noted that, because of the convex shape of the velocity profile in the vortex interior, the topographic features needed for stability are quite tall for Gaussian vortices (for a vortex with Ro = −0.3 and large Burger number, $\tilde{h}_b$ is already comparable to H).

A simple extension of the Gaussian profile, whose stability was examined by Stegner and Dritschel (2000), is given by

$$v = x\exp\left[\frac{1}{\alpha}(1-x^\alpha)\right], \quad \zeta = \zeta_0\left(1-\frac{x^\alpha}{2}\right)\exp\left(-\frac{1}{\alpha}x^\alpha\right), \tag{18}$$

with $\zeta_0 = 2\omega_m e^{1/\alpha}$. These profiles were introduced in Carton et al. (1989) and have also been studied in the context of two-layer SWE over a flat bottom, in a recent work by Baey and Carton (2002), focusing on the formation of long-lived tripolar structures. For $\alpha > 2$, (18) yields vorticity profiles steeper than that of the Gaussian vortex ($\alpha = 2$). However, the expression of ζ_0 shows that the dynamical Rossby number decreases with increasing

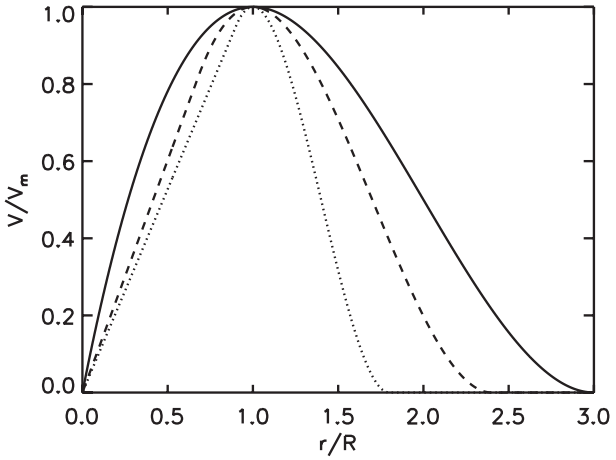

FIG. 2. The linear-cubic velocity profile of Eq. (22) for three different vortex sizes [$\beta = 1.8$ (dotted), 2.4 (dashed), and 3 (solid)].

α (it tends toward a limiting value of $2\omega_m/f$). Thus, for given Rossby and Burger numbers, the size of the stabilizing topography tends to be smaller at larger α.

Smaller topographic features are also obtained by taking a linear velocity profile in the vortex core, consistent with observations of mesoscale oceanic vortices (see Paldor 1999). The problem with a linear profile is that it must be matched with an external profile that allows for the rapid decay usually observed beyond the radius of maximum speed. This requires some care, because the simplest solution (i.e., matching the linear profile at $r = R$ with an exponentially or power-law-like decaying external one) leads to global profiles with a vorticity jump that are prone to instability (Paldor 1999). To avoid these discontinuities, we match the inner linear profile V_I at a radius $r = a < R$ with an exterior profile V_E, defined by a cubic polynomial in r, with coefficients chosen so that both V and dV/dr are continuous at $r = a$ and vanish at a radius $r = b > R$. If ω is the rotation frequency in the vortex core, the external profile is given by

$$V_E(x) = \frac{\omega R}{(\beta - \alpha)^3} \sum_{i=0}^{3} c_i x^i, \tag{19}$$

with $\alpha \equiv a/R$, $\beta \equiv b/R$, and

$$c_0 = -2\beta^2\alpha^2, \quad c_1 = \beta(\beta^2 + \alpha\beta + 4\alpha^2)$$
$$c_2 = -2(\beta^2 + \alpha\beta + \alpha^2), \quad c_3 = \beta + \alpha. \tag{20}$$

Asking that $V_E(1) = V_m$ yields

$$\omega = \frac{V_m}{R} \frac{(\beta - \alpha)^3}{\sum_{i=0}^{3} c_i}, \tag{21}$$

and consequently the normalized profile

$$v_I = \frac{(\beta - \alpha)^3}{\sum_{i=0}^{3} c_i} x, \quad v_E = \frac{\sum_{i=0}^{3} c_i x^i}{\sum_{i=0}^{3} c_i}. \tag{22}$$

Finally, the condition $dv_E/dx(1) = 0$ gives an algebraic relation between α and β, which can be solved for α to find

$$\alpha = \frac{1}{8}[3 - \beta + \sqrt{(3 - \beta)(3 + 15\beta)}]. \tag{23}$$

Once this expression is placed in (22), the velocity profile is completely specified in terms of the only free parameter remaining, the vortex size β. It should be noted that (23) implies $\beta \leq 3$: that is, the size of the vortex cannot exceed 3 times the radius of maximum speed. This result, not obvious a priori, is interesting, since many oceanic vortices studied in the literature tend to be of this size or smaller.

The normalized velocity profile (22) is shown in Fig. 2 for different vortex sizes ($\beta = 1.8$, 2.4, and 3). The bounding profile with $\beta = 3$ has $\alpha = 0$ (i.e., it has no linear region at all, although it is approximately linear at small r) and takes the simple form $v = x(3 - x)^2/4$. The $\tilde{h}_b$ profiles for the case $\beta = 2.4$ and the same parameters of Fig. 1 are shown in Fig. 3 along with the corresponding modified profiles (dashed lines), with $\epsilon = -0.05$. As expected, the sizes of the topographic features are significantly smaller than for the Gaussian profiles and would further approach $2\omega_m/f$ for smaller size vortices (not shown) with more ''triangular'' velocity profiles.

Trying to further reduce the topography size, we have also considered some slightly concave velocity profiles in the vortex interior. This allows smaller values of $\tilde{h}_b/H$ in the core, but values slightly higher than $2\omega_m/f$ are found just to the left of the radius of maximum speed because of the stronger velocity gradient in that region (with respect to the linear case). We have not been able to obtain marginal topographic features of size smaller than $2\omega_m/f$.

3. 2D SW vortices

We now briefly consider the extension of the previous approach to the case in which both the vortex and the topography are fully two dimensional. The 2D SW equilibrium system reads

$$(\zeta + f)\mathbf{k} \times \mathbf{v} = -\nabla\left(gh + gh_b + \frac{1}{2}v^2\right) \equiv -\nabla B \quad \text{and} \tag{24}$$

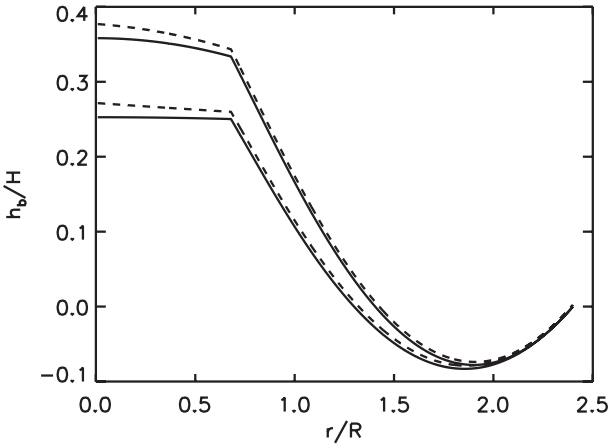

FIG. 3. As in Fig. 1, but the velocity profiles are of the form (22), with $\beta = 2.4$.

$$\nabla \cdot (h\mathbf{v}) = 0, \tag{25}$$

where B is the Bernoulli function. The continuity Eq. (25) can be satisfied by introducing a transport streamfunction ψ such that $h\mathbf{v} = \mathbf{k} \times \nabla\psi$. Then, it follows from (24) that B is a function of ψ and that $q = q(\psi) = dB/d\psi$. Consequently, the equilibrium problem reduces to two coupled equations for ψ and h,

$$\nabla \cdot \left(\frac{1}{h}\nabla\psi\right) = -f + hq(\psi) \quad \text{and} \tag{26}$$

$$\frac{1}{2}|\mathbf{v}|^2 + gh + gh_b = B(\psi), \tag{27}$$

which must be solved for a $q(\psi)$ of interest. The functional relation between q and ψ has direct bearing on stability, since for 2D flows Ripa's condition becomes

$$\frac{dq}{d\psi} > 0, \quad |\mathbf{v}|^2 < gh \tag{28}$$

everywhere.

Now consider a vortex with constant PV, $q = \tilde{q}$, and consequently linear Bernoulli function, $B = B_0 + \tilde{q}\psi$, with B_0 as a constant. Differently from the axisymmetric case, we cannot arbitrarily choose the velocity field for this vortex; using (3) to express h in terms of ζ and $\tilde{q}$ and placing the result in (25) gives a complicated relation that $\mathbf{v}$ has to satisfy. Instead, we may choose the form of ψ, solve (26) for h, compute the velocity field, and place the results in (27), which becomes a definition of the marginal topography. Eliminating h in favor of ζ gives

$$h_b = -\frac{1}{\tilde{q}}\zeta - \frac{|\mathbf{v}|^2}{2g} + \frac{\tilde{q}}{g}\psi \tag{29}$$

(here, we have let ψ go to zero for $\mathbf{r} \to \infty$ and taken $B_0 = fg/\tilde{q}$ so that h_b also vanishes in the same limit).

Let us assume we have carried out this procedure, and let $\tilde{\psi}$, $\tilde{h}$, $\tilde{h}_b$ be the fields that characterize the constant-PV vortex. Then, just as in the axisymmetric case, we can consider a new vortex with the same velocity field and the same free surface [which is still solution of (24)] but with topography and fluid depth modified as in (9) and with γ being a two-dimensional function of position. From (25), we find the constraint

$$\mathbf{v} \cdot \nabla\left(\frac{\gamma}{\tilde{h}}\right) = 0, \tag{30}$$

which is satisfied by taking

$$\gamma = \tilde{h}F(\tilde{\psi}), \tag{31}$$

with F as an arbitrary function of $\tilde{\psi}$. The PV of the modified vortex is

$$q = q(\tilde{\psi}) = \tilde{q}\frac{1}{1 - F(\tilde{\psi})}, \tag{32}$$

and its streamfunction ψ is given by

$$\frac{d\psi}{d\tilde{\psi}} = \frac{1}{1 - F(\tilde{\psi})}. \tag{33}$$

Consequently,

$$\frac{dq}{d\psi} = q\frac{dF}{d\tilde{\psi}}, \tag{34}$$

which shows that, to satisfy Ripa's condition, it is sufficient to choose a monotonically increasing $F(\tilde{\psi})$ (note that, since $\tilde{h}$ is generally not a function of $\tilde{\psi}$, the resulting γ will not be a function of $\tilde{\psi}$; i.e., the topographic contours of the stable vortex and of the constant-PV vortex will have different shapes).

The previous considerations indicate that 2D SW vortices over topography satisfying Ripa's condition may be constructed following a procedure similar to the one adopted in the axisymmetric case. Further work is needed, however, to address the difficulties related to the choice of the starting streamfunction and to the numerical solution of the partial differential Eq. (26).

4. Conclusions

The main result of the present work is the analytic construction of isolated, axisymmetric SW vortices over topography that satisfy Ripa's (1987) stability criterion.

To our knowledge, this is the first exact stability result concerning SW vortices with realistic velocity profiles; previous analytic studies were restricted to quite special equilibrium flows, such as the constant-PV vortex with a discontinuity at its boundary analyzed by Ford (1994) or the rotating elliptic vortex (Rodons) introduced by Cushman-Roisin et al. (1985), whose stability was studied in Ripa (1987), which has been the starting point of our investigation.

We have examined velocity profiles representative of those observed in mesoscale oceanic vortices, showing that, at large Burger numbers (i.e., for small-size vortices), these profiles can be stabilized by topographic features with radial sizes comparable with that of the vortex (about twice the radius of maximum speed) and maximum vertical size (normalized to the unperturbed fluid depth) from 2 to 3.3 times the Rossby number ω_m/f (the upper limit holding for Gaussian profiles). Although results of single-layer theory should be used with caution when discussing geophysical vortices, we believe that examples of this stabilization mechanism are likely to be found in real oceanic contexts.

Our construction of stable, axisymmetric SW equilibria relies on first computing the topography that makes the velocity profile in consideration a constant-PV solution of the SWE and then modifying this topography (and the corresponding fluid depth profile) so as to have new steady solutions with monotonic PV that satisfy Ripa's stability condition. We have argued that a similar approach, albeit more involved and partly numerical, could be used to construct stable 2D SW vortices over 2D topography. Such a construction is left for future work.

The SW stability results are not in contradiction with those of NL04, since we also find stable anticyclones (cyclones) over elevations (depressions). This is because the topography that yields constant-PV (the ''marginal topography'') is hill-like (valley-like) for anticyclones (cyclones) and because the alterations of this topography needed to satisfy Ripa's condition cannot change its global shape (i.e., cannot transform hills in valleys or vice versa). It should be kept in mind, however, that Ripa's criterion is only a sufficient condition for stability and that its violation does not imply instability. As a consequence, we cannot exclude the existence of stable equilibria with nonmonotonic PV or with a PV gradient of opposite sign. The latter would correspond to negative $dq/d\psi$ and could be obtained with topographic corrections of opposite sign than those considered in section 2. Such corrections could change the global shape of the topography.

In fact, since in the absence of topography both cyclones and anticyclones have negative $dq/d\psi$ in the region of maximum speed and in many cases over most of the vortex, SW steady states with uniformly negative $dq/d\psi$ would require the presence of modest topographic features. On the other hand, anticyclones (cyclones) over depressions (elevations) of the sizes we have previously considered would tend to have strongly negative $dq/d\psi$. Existence of stable solutions of this kind would definitely yield a more complex and intriguing stability picture.

The idea of a second stability region, for SW flows with strongly negative $dq/d\psi$, analogous to that existing for Euler flows (Arnold 1966), is not new. Support for this idea comes, for example, from the numerical investigation of the stability of Jupiter's zonal winds performed by Dowling (1993). To date, however, a SW analog of Arnold's second stability theorem is still lacking, and the existence of such equilibria in our context could only be explored numerically.

A final word of caution should concern the small-amplitude nature of Ripa's criterion. Although formally similar to Arnold's first stability theorem for Euler flows, Ripa's condition does not hold in the fully nonlinear case; the structure of the SWE seems to prevent its extension to finite-amplitude perturbations. In absence of analytic progress on the matter, this is another point that should be tested numerically to verify whether the stabilization by topography we have explored also works in the nonlinear regime.

REFERENCES

Arnold, V. I., 1966: On an a priori estimate in the theory of hydrodynamical stability. *Izv. Vyssh. Uchebn. Zaved. Mat.,* **54,** 3–5.

Baey, J. M., and X. Carton, 2002: Vortex multipoles in two-layer rotating shallow-water flows. *J. Fluid Mech.,* **460,** 151–175.

Benilov, E. S., 2005: Stability of a two-layer quasigeostrophic vortex over axisymmetric localized topography. *J. Phys. Oceanogr.,* **35,** 123–130.

Carnevale, G. F., and J. S. Frederiksen, 1987: Nonlinear stability and statistical mechanics of flow over topography. *J. Fluid Mech.,* **175,** 157–181.

Carton, X., G. R. Flierl, and L. Polvani, 1989: The generation of tripoles from unstable axisymmetric isolated vortex structures. *Europhys. Lett.,* **9,** 339–344.

Cushman-Roisin, B., W. H. Heil, and D. Nof, 1985: Oscillations and rotations of elliptical warm-core rings. *J. Geophys. Res.,* **90** (C6), 11 756–11 764.

Dowling, T. E., 1993: A relationship between potential vorticity and zonal wind on Jupiter. *J. Atmos. Sci.,* **50,** 14–22.

Ford, R., 1994: The instability of an axisymmetric vortex with monotonic potential vorticity in rotating shallow water. *J. Fluid Mech.,* **280,** 303–334.

Kunze, E. S., and J. M. Toole, 1997: Tidally driven vorticity, diurnal shear, and turbulence atop Fieberling Seamount. *J. Phys. Oceanogr.,* **27,** 2663–2693.

Nore, C., and T. G. Shepherd, 1997: A Hamiltonian weak-wave model for shallow-water flow. *Proc. Roy. Soc. London,* **453A,** 563–580.

Nycander, J., and J. H. LaCasce, 2004: Stable and unstable vortices attached to seamounts. *J. Fluid Mech.,* **507,** 71–94.

Paillet, J., B. Le Cann, X. Carton, Y. Morel, and A. Serpette, 2002: Dynamics and evolution of a northern meddy. *J. Phys. Oceanogr.,* **32,** 55–79.

Paldor, N., 1999: Linear instability of barotropic submesoscale coherent vortices observed in the ocean. *J. Phys. Oceanogr.,* **29,** 1442–1452.

Ren, S., and T. G. Shepherd, 1997: Lateral boundary contributions to wave-activity invariants and nonlinear stability theorems for balanced dynamics. *J. Fluid Mech.,* **345,** 287–305.

Ripa, P., 1987: On the stability of elliptical vortex solutions of the shallow-water equations. *J. Fluid Mech.,* **183,** 343–363.

Salmon, R., 1983: Practical use of Hamilton's principle. *J. Fluid Mech.,* **132,** 431–444.

Stegner, A., and D. G. Dritschel, 2000: A numerical investigation of the stability of isolated shallow water vortices. *J. Phys. Oceanogr.,* **30,** 2562–2573.